with fewer magnet rings or nonmagnetic discharge chambers may not be so great.

Summary

Efforts to reduce thruster mass through the reduction in the number of discharge chamber magnets and the removal of discharge chamber magnetic material can lead to a reduction in the intercusp magnetic field at the anode. Reductions in the containment capability of the intercusp magnetic field could lead to degradation in thruster performance. To address this issue, electron transport to the anode at the intercusp regions was investigated in an NSTAR-derivative ion thruster. Intercusp electron flow to the NSTAR-derivative ion thruster anode as measured at wall probes located between magnetic cusps was found to be classical. Additionally, based on this finding, it should be possible to calculate the magnitude of electron current lost between cusps provided the average magnetic field and local plasma properties between cusps are known.

Acknowledgments

The author would like to thank George Soulas, Michael Patterson, Robert Roman, and James Sovey for assistance in carrying out this work.

Reference

[1]Sovey, J. S., "Improved Ion Containment Using a Ring-Cusp Ion Thruster," *Journal of Spacecraft and Rockets*, Vol. 21, No. 5, 1984, pp. 488–495.

[2]Hershkowitz, N., Leung, K. N., and Romesser, T., "Plasma Leakage Through a Low-Beta Line Cusp," *Physical Review Letters*, Vol. 35, No. 5, 1975, pp. 277–280.

[3]Arakawa, Y., Hamatani, C., and Kawasaki, Y., "Wall Losses of Charge Particles in a Multipole Discharge Plasma," *International Electric Propulsion Conference*, IEPC Paper 84-69, 1989.

[4]Horiike, H., Akiba, M., Ohara, Y., Okumura, Y., and Tanaka, S., "Cusp Width and Power Flow Study at a High Power Magnetic Multipole Source," *Physics of Fluids*, Vol. 30, No. 10, 1987, pp. 3268–3275.

[5]Beattie, J., and Matossian, J., "Mercury Ion Thruster Technology," NASA CR-174974, March 1989, pp. 30–50.

[6]Patterson, M. J., Haag, T. W., and Hovan, S. A., "Performance of the NASA 30 cm Ion Thruster," *International Electric Propulsion Conference*, IEPC Paper 93-108, 1993.

[7]Noci, G., Capacci, M., Redaelli, R., Matucci, A., Matticari, G., Severi, A., and Sabbagh, J., "Development of Small Ion Thrusters for Lightsats Applications," AIAA Paper 95-3071, 10–12 July 1995.

[8]Brophy, J. R., "Advanced Ion Propulsion Technology for Solar System Exploration," AIAA Paper 97-2782, 6–9 July 1997.

[9]Patterson, M. J., and Oleson, S. R., "Low Power Ion Propulsion for Small Spacecraft," AIAA Paper 97-3060, 6–9 July 1997.

[10]Patterson, M. J., "Low-Power Ion Thruster Development Status," AIAA Paper 98-3347, 13–15 July 1998.

[11]Christensen, J. A., Freick, K. J., Hamel, D. J., Hart, S. L., Norenberg, K. T., Haag, T. W., Patterson, M. J., Rawlin, V. K., Sovey, J. S., and Anderson, J. R., "Design and Fabrication of a Flight Model 2.3 kW Ion Thruster for the Deep Space 1 Mission," AIAA Paper 98-3327, 13–15 July 1998.

[12]Sovey, J. S., Hamley, J. A., Haag, T. W., Patterson, M. J., Pencil, E. J., Peterson, T. T., Pinero, L. R., Power, J. L., Rawlin, V. K., Sarmiento, C. J., Anderson, J. R., Bond, T. A., Cardwell, G. I., and Christensen, J. A., "Development of an Ion Thruster and Power Processor for New Millenium's Deep Space 1 Mission," AIAA Paper 97-2778, 6–9 July 1997.

[13]Hutchinson, I. H., *Principles of Plasma Diagnostics*, Cambridge Univ. Press, New York, 1987, pp. 66–71.

[14]Sugawara, M., "Electron Probe Current in a Magnetized Plasma," *Physics of Fluids*, Vol. 9, No. 4, 1966, pp. 797–800.

[15]Taylor, J. R., *An Introduction to Error Analysis*, Oxford Univ. Press, Mill Valley, CA, 1982, pp. 40–80.

[16]Foster, J. E., Soulas, G. C., and Patterson, M. J., "Plume and Discharge Measurements of an NSTAR-Type Ion Thruster," AIAA Paper 2000-3812, 16–19 July 2000.

[17]Chen, F., *Introduction to Plasma Physics and Controlled Fusion*, Plenum, New York, 1984, pp. 169–174, 190–195.

[18]Bohm, D., "Qualitative Description of the Arc Plasma in a Magnetic Field," *The Characteristics of Electrical Discharges in Magnetic Fields*, edited by A. Guthrie and R. K. Wakerling, McGraw–Hill, New York, 1949, pp. 1–12.

[19]Kaufman, H. R., and Robinson, R. S., *Operation of Broad Beam Ion Sources*, Commonwealth Scientific, Alexandria, VA, 1984, pp. 137–141, 142–144.

Optimal Three-Dimensional Nozzle Shape Design Using CFD and Parallel Simulated Annealing

X. Wang* and M. Damodaran†
Nanyang Technological University, Singapore 639798, Republic of Singapore

Introduction

COMPUTATIONAL methods, which are implemented for optimizing aerodynamic shape within the framework of complex single/multidisciplinary optimization design (MDO), are becoming popular in recent years. Most of the current methods of optimization can generally be classified into two distinct groups, namely deterministic and stochastic approaches. Deterministic optimization methods, such as the gradient-based methods and sensitivity analysis, have been favored by many researchers such as Frank et al.[1] One salient feature of gradient-based methods is that they are very efficient in finding the minima of continuously differentiable problems, where sufficiently accurate derivatives can be obtained at reasonable cost. The sensitivity analysis methods have been used in aerodynamic shape design and MDO extensively in recent years; however, sensitivity information cannot be easily extracted from computational fluid dynamics (CFD) codes, and this poses the main obstacle for using gradient-based methods in developing tightly coupled solution methods for MDO. Deterministic methods also largely increase the work of constructing sensitivity analysis models in design problems using CFD. Stochastic optimization methods that are quite robust in searching for the global optimum, such as simulated annealing (SA), genetic algorithm (GA), and genetic simulated annealing (GSA) method, are also being used as nontraditional optimization methods in engineering and scientific research for single and multidisciplinary design optimization. Parallel versions of these algorithms have been extensively applied to solve practical engineering problems for enhancing performance of these approaches and reducing computational overburden in large number of evaluations of the objective function. A survey of parallel simulated annealing (PSA) has been detailed by Aarts and Korst.[2] Further work on these PSA have been done by Diekmann et al.[3] and Gallego et al.[4] Parallel genetic algorithms (PGA) has also attracted attention for its inherent property of parallelization. The basic idea for GA in optimization was introduced by Goldberg.[5] Different forms of implementations of PGA have been outlined by Bianchini and Brown[6] and Cantú-Paz.[7] Doorly et al.[8] have successfully applied a PGA to the problem in aeronautical design optimization. The goal of the present study is to use computational fluid dynamics methods with PSA for global optimization in the design space as described in Wang and Damodaran[9] and in which PSA has been shown to be a suitable tool for reducing wall-clock time for the design of two-dimensional and axisymmetric design problems on coarse-gained processors. In this study the

Received 2 January 2001; revision received 11 June 2001; accepted for publication 3 July 2001.

*Research Fellow, Center for Advanced Numerical Engineering Simulations, Nanyang Avenue. Member AIAA.

†Associate Professor, School of Mechanical and Production Engineering, Center for Advanced Numerical Engineering Simulations, Nanyang Avenue. Senior Member AIAA.

method is applied to three-dimensional design problems. The test problem chosen to illustrate this aspect concerns the search for the optimal three-dimensional shape of the nozzle, which maximizes the thrust of the nozzle. The three-dimensional CFD solver for solving the Euler and Navier–Stokes equations is used to compute the internal flowfield from which the objective function is evaluated for each iterated aerodynamic shape. The feasibility of using PSA optimization method for three-dimensional aerodynamic shape design optimization problem is considered. The speedup and efficiency of the parallel implementations have also been investigated in the course of the study. The simulation and optimization has been implemented on a shared memory SGI Origin 2000 architecture with multiple processors and using Message Passing Interface (MPI) library on the machine to parallelize the optimization algorithm.

CFD Models for Estimating Objective Functions

Three-dimensional high-speed internal flow systems are of interest in this aerodynamic shape design studies. A three-dimensional compressible CFD solver for solving the Reynolds-averaged Euler/Navier–Stokes equations is developed to compute the flowfield in which converged steady-state solutions are obtained by time-marching scheme from the initial conditions. The computed flowfield is then used to estimate the objective function that is to be optimized. To enhance convergence, these equations are solved using the LU-SGS implicit scheme proposed by Yoon and Kwak.[10] To improve the resolution of the computed flowfield, the total variation diminishing (TVD) scheme proposed by Yee and Harten[11] is implemented.

Parallel Simulated Algorithms for Optimization

Simulated annealing is an heuristic strategy for obtaining near-optimal solutions and derives its name from an analogy to the annealing of solids. The essential features of the basic SA method for optimizing complex engineering problems are outlined in Aarts and Korst.[2] One shortcoming of the SA is the enormous expenditure of computational resources for objective function evaluations when used in optimizing a large number of design variables of complex engineering problems comparing with the gradient-based method. In view of this feature, the current investigation addresses the issue of developing robust computational methods for using PSA in conjunction with CFD, which is used for evaluating the design objective functions for the selected design problems in aerodynamics area. Several different parallel schemes of SA have been discussed by Bhandarkar and Machaka[12]; other variants include the systolic method by Laarhoven and Aarts,[13] the speculative method by Witte and Franklin,[14] and divisions algorithm by Aarts and Korst.[2] In present investigation of PSA, the divisions algorithm and clustered method are combined together as in the strategies of Diekmann et al.[3] The divisions algorithm is carried out by dividing a Markov main chain into subchains on the multiple processors. The clustered method is an efficient method at lower temperature as mentioned by Bhandarkar and Machaka.[12] A full discussion of preceding algorithms is given in Wang and Damodaran.[9]

Design Optimization of Three-Dimensional Nozzle Shape

Aerodynamic shape design combining modern CFD and optimization methods has potential applications in the design of airfoils and wings, flight vehicles, aerospike, wind tunnels, nozzles, diffusers, and jet engine components. The design test case chosen for the application of PSA for optimum aerodynamic shape design concerns the optimal design of a three-dimensional elliptical nozzle shape. The elliptical nozzle is chosen because it is relatively simple to model and can be viewed as having applications in integral rocket-ramjet, scramjet, and high-speed internal flow systems. To initiate the design process, there is a need for the parametric representation of the surfaces of the three-dimensional nozzle shape. A number of choices exist for this. One choice would be to use cubic splines to define surfaces and design parameters for the shape design. Cubic splines produce an interpolated function, which preserves continuity in its second derivative and smoothness in its first derivative. For the three-dimensional shape design studied in this work, bicubic splines that interpolate one functional value alone first and that then interpolate another functional value are used to define the design variables and the shape of the surface in the three-dimensional space. Details of this procedure are outlined in Press et al.[15] In this study the natural cubic spline, which has zero second derivative at the inlet and outlet boundaries of the nozzle configuration, is chosen. The test case is designed for optimizing the shape of a three-dimensional elliptical nozzle for which the inflow flowfield conditions are defined. The goal is to find an optimal shape of the nozzle wall or cross-sectional area distribution along the flow direction to maximize the thrust of nozzle. The objective function that has to be optimized is expressed in normalized form

$$F(X) = \int \frac{\rho u^2 + p}{\rho_0 u_0^2} \, \mathrm{d}S$$

where the $\mathrm{d}S$ equals to $\mathrm{d}y\,\mathrm{d}z$ on the exit cross section $\rho_0 u_0^2$, where ρ_0 and u_0 are the inflow density and velocity respectively that are taken as reference values for scaling flow quantities in internal flow simulations using CFD analysis and X is the vector of design variables, i.e., $X = (x_1, x_2, \ldots, x_{16})$. The integration is evaluated on the cross section of nozzle exit. The flowfield is calculated by numerically solving the Euler equations on a structured three-dimensional grid consisting of 71 points in the axial direction and 15 points each in the radial and circumferential directions. The inflow Mach number is set at 1.1, and supersonic inflow and outflow boundary conditions are specified. The cross-sectional areas at inlet, throat, and outlet are fixed in the optimization process and are set to be ellipses. The inlet cross-sectional shape is defined by selecting the ratio of the major axis to the minor axis to be $b/a = 0.5/1.0$, and for the throat and outlet their ratio is 0.45/0.90 and 1.0/2.0, respectively. In the design optimization process the design surface nodes are constrained not to move axially along the length of the nozzle and are also fixed in the circumferential direction along the 0-, 30-, 60-, and 90-deg rays emanating from the center of the nozzle section. The 16 points are free to move along the radial direction and are grouped into four cross-sectional planes, which are uniformly located along length of nozzle. The radii R_i $(i = 1, 16)$ denoted in Fig. 1 are the control points on the surface of the nozzle, which are defined as the design variables to be optimized. In this study the design variables are only subjected to predefined upper and lower limits. By monitoring the results on multiple processors, the efficiency of the PSA can be evaluated. Additional computation is done for examining the efficiency of the PSA using the full Navier–Stokes equations on a grid comprising of 51 points in the axial direction and 25 points each in the radial and circumferential direction for simulating turbulent flows with a simple algebraic turbulence model. The motivation for reducing the number of grid points in the axial direction and increasing the number of grid points in the other two directions is to adequately

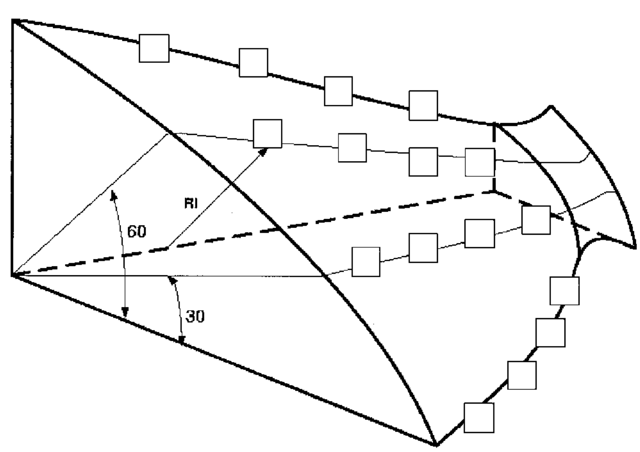

Fig. 1 Design variables in three-dimensional nozzle design (one quadrant).

resolve viscous effects on the radial and circumferential directions while maintaining the same number of grid points as in inviscid case so as not to increase computational time encountered in the simulation of viscous flows and because this test case is to demonstrate the integration of CFD and optimization ideas in a parallel computing environment. Also because a high-resolution TVD-type numerical scheme is used, it is felt that viscous effects can be adequately resolved even on the modest grid sizes that are used in this study. The Reynolds number Re is $1.4E+7$ based on the characteristic length of major axis of the elliptical cross section at the inlet. The parameters of the inflow and initial geometry of the nozzle are all the same as those pertaining to the nozzle used for inviscid flow analysis. Based on the efficiency of the parallel computing in the inviscid flow design and processors available for computation, eight processors have been chosen for the optimal design considering turbulent flows.

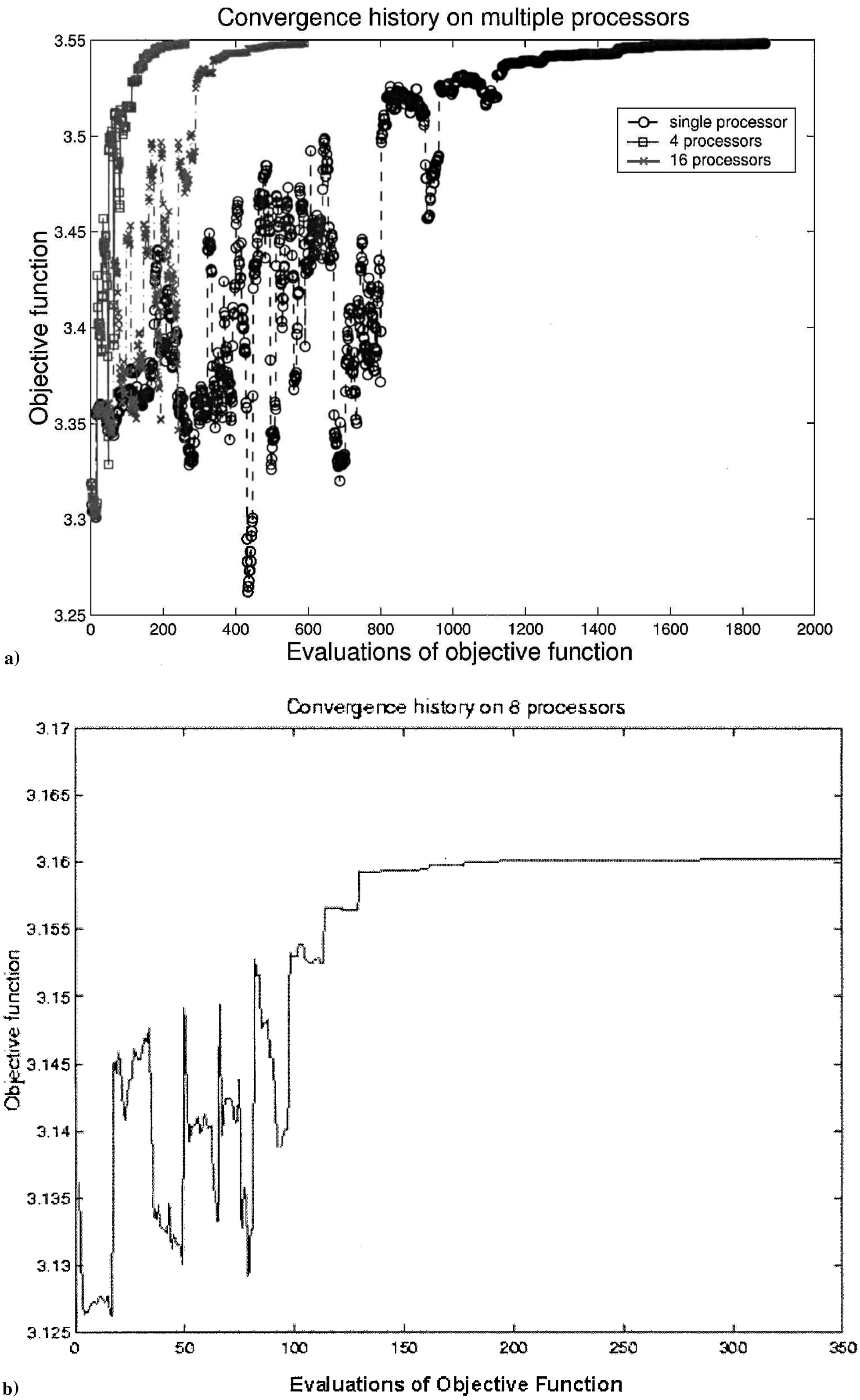

Fig. 2 Variation of objective function with number of function evaluations corresponding to an a) inviscid flow model on 1, 4, 16 processors and a b) viscous turbulent flow model on eight processors.

Results and Discussions

In this study the PSA tuning parameters are chosen such that the initial cooling temperature is set to a value at which the initial cooling acceptance ratio is greater than 0.95. The main length for the cooling scheme is first tested and then taken to be as short as possible on a single processor. The length of the main chain is chosen to be $10n$, where n is the number of the design variables. A constant cooling scheme $T_{k+1} = \alpha T_k$ is chosen with $\alpha = 0.15$. The termination criteria (for inviscid flow) to stop the program is if the maximum thrust of 3.548 is attained, and this can be defined in the sense of a minimization problem as that of the objective function reaching a value, which is less than $F_{\min} = 1/3.548$ based on the results collected from all the processors. Figure 2a shows the convergence histories of the objective function as it reaches the maximum value from its initial values pertaining to PSA implementations on different combinations of processors on 1, 4, and 16 processors. All convergence histories on multiprocessors are plotted from the results of processor number 0 only for the convenience of comparison. The converged values of

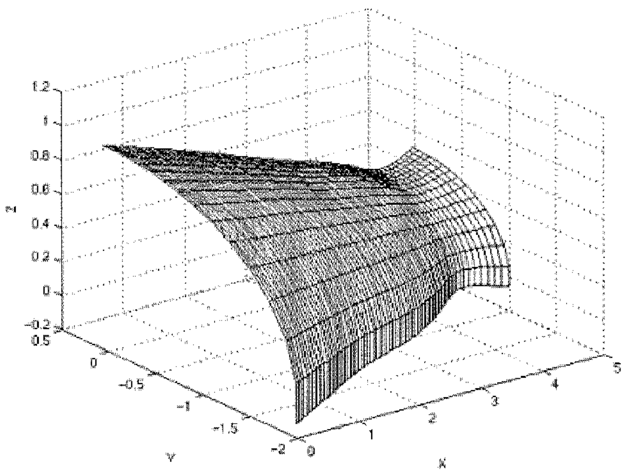

a) Initial shape (view of a quadrant of the nozzle)

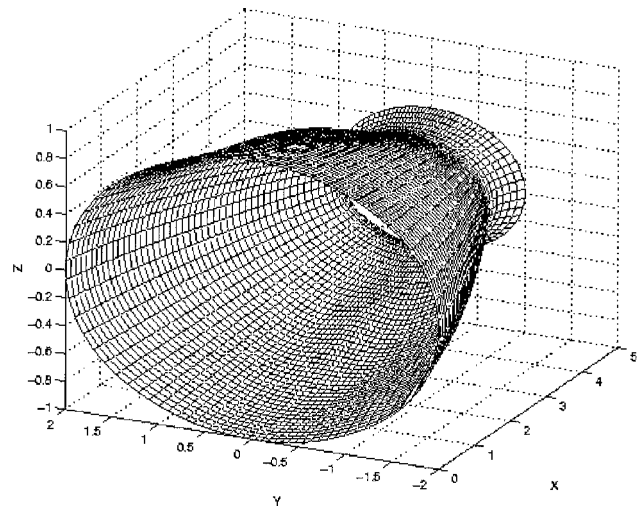

c) Optimized shape (viscous turbulent case; view of the full nozzle)

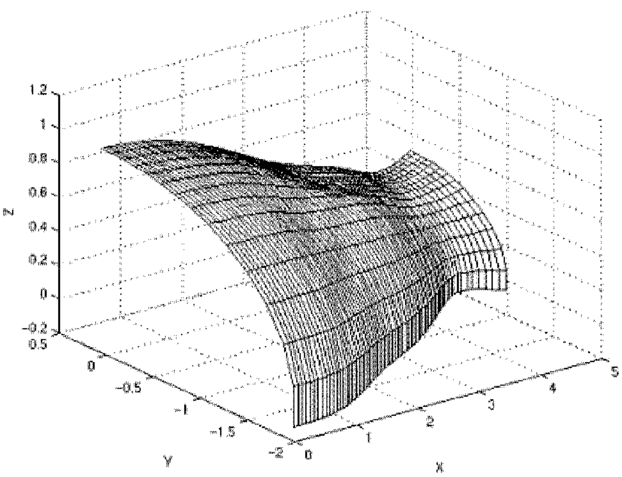

b) Optimized shape (inviscid case; view of a quadrant of the nozzle)

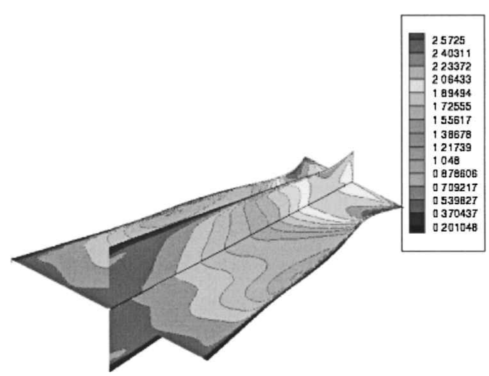

d) Initial distribution of the dynamic pressure (viscous turbulent flow)

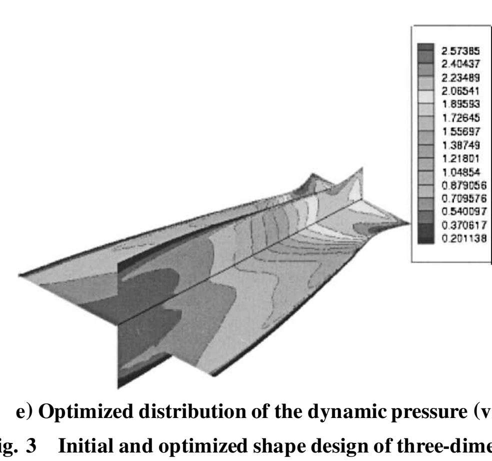

e) Optimized distribution of the dynamic pressure (viscous turbulent flow)

Fig. 3 Initial and optimized shape design of three-dimensional elliptical nozzles.

the objective function are reached with fewer iterations while using multiprocessors compared with that obtained on single processor. It can be seen that the number of evaluations of objective function on multiple processors to reach the final optimal design shape according to the termination criteria has reduced remarkably from 1823 on single processor to 260 on 16 processors. The wall-clock time indicates a reduction from 125 h on single processor to around 18 h on 16 processors and 17 h on 24 processors. The speedup registered are 1.9, 3.15, 4.9, 7.2, and 7.7 corresponding to 2, 4, 8, 16, and 24 processors, respectively. It appears that the PSA algorithm shows reasonable speed up for the three-dimensional nozzle design problem if one to eight processors are used in the computational task and also registers a reduction in the wall-clock time from 125 to 26 h. This also shows that using 16 processors would be sufficient as the usage of 24 processors result in only marginal benefits as the wall-clock time has reduced to 18 h. The reason is that by increasing the number of processors the length of the chain is reduced to a limit value, on which performance of PSA will no longer be enhanced. Design results corresponding to the use of Navier–Stokes solver for turbulent flow in Fig. 2b shows the convergence histories of the objective function as it reaches the maximum value from its initial values pertaining to PSA implementations on eight processors. The total wall-clock time is 223 h with 350 evaluations of the objective function. Corresponding to the case of inviscid flow design on eight processors, if single processor is used then about 1000 h wall-clock time might be expected for the computation of the viscous flow design. The convergence history in Fig. 2b shows that converged result is achieved even starting from 200 function evaluations. On the basis of this computation, it can be seen that the maximum thrust of the nozzle attained by the viscous design is slightly lower than the value attained by inviscid design, which is closer to the specified value. This could possibly be overcome by using improved turbulence models capable of resolving the three-dimensional boundary layers that develop on the nozzle walls and by increasing the grid points and can form a separate study in the near future. Figure 3 shows the optimized shape of the whole three-dimensional nozzle that evolved from the initial configuration shown in Fig. 3a to final optimized shape in Fig. 3b for inviscid flow and Fig. 3c for turbulent flow. Figures 3d and 3e compare the contours of the distribution of the quantity $(\rho u^2 + p)/(\rho_0 u_0^2)$ on the cross-sectional planes located at $X = 0$, 1.2, and 2.2 for the initial configuration of the nozzle and the optimized configuration of the nozzle under consideration of turbulent flow. As there are a variety of approaches to define the shape functions to describe the evolving three-dimensional geometric shape, we feel that this might have influenced the occurrence of the ridge along $y = 0$ creating nonconventional wall contours as can be seen from Figs. 3c and 3e. In this work 16 design variables (16 radial positions) emanating from the axis $y = 0$ equally spaced along the $y = 0$ axis and at equally spaced angular positions in the circumferential direction at each plane along the axis have been used for shape representation of the nozzle using bicubic splines. Besides this choice, there are many possible arrangements for example distributing the points with unequal spacing instead of equal spacing along the angular direction. Alternatively, more points (implying more design variables and hence more computational costs) could be used instead of the current 16 to optimize the shape, and the ridge might not be present at all. Also the slightly lower value of the attained thrust by using the viscous turbulent model may suggest that the true optimized shape might not have been reached under the current combination of the grid points, parametric definition of the surfaces, etc. Hence this could also be one reason for the occurrence of the ridge suggesting that the solution is not the global optimal solution that would have been captured but somewhat closer to the global optimal solution corresponding to the shape delivering the maximum thrust. As the primary aim of this work is to demonstrate the combination of PSA, CFD, and parallel computing on nozzle design problems, the present work has not focused on the impact of various methods for geometric surface definitions on the optimized result. The impact of different methods for geometric shape definitions for the three-dimensional shapes such as NURBS, Bezier Surface Patches, bicubic splines, etc., on the optimized solution requires further study and will be carried out in due course as a separate study and reported as a companion Note in the future.

Conclusions

Design optimization of the three-dimensional aerodynamic shape of high-speed internal flow systems using CFD methods for Euler and Navier–Stokes equations and parallel SA algorithms have been implemented on multiple processors in this study. The computed results show that parallel simulated annealing (PSA) appears to be a robust and simple approach for the design of complex problems such as three-dimensional aerodynamics on coarse-grained parallel computer and that the evaluations of objective function can be reduced to the same level as generic gradient-based methods. A reasonable number of processors can be used in the implementation of PSA for achieving satisfactory speed up and efficiency. In the current work a relatively coarse grid system is used for the case study considering simplicity and for feasibility demonstration purposes. The impact of viscous effects should be considered with finer grids and improved turbulence models in the context of high-resolution numerical schemes in practical applications. The impact of the choices of parametric surface definition of the nozzle geometrical shape on the evolution of optimized shape should also be considered in the context of this work. In addition to addressing these impacts, in the future the optimization method based on combining an adaptive SA and hybrid optimizer will be explored to further enhance the performance of SA.

Reference

[1]Frank, P. D., Booker, A. J., Caudel, T. P., and Healy, M. J., "Optimization and Search Methods for Multidisciplinary Design," AIAA Paper 92-4827, *4th Symposium on Multidisciplinary Analysis and Optimization*, Cleveland, OH, 21–23 Sept. 1992.

[2]Aarts, E., and Korst, J., *Simulated Annealing and Boltzmann Machines, A Stochastic Approach to Combinatorial Optimization and Neural Computing*, Wiley, New York, 1989, pp. 13–114.

[3]Diekmann, R., Luling, R., and Simon, J., "Problem Independent Distribution Simulated Annealing and Its Applications," *Lecture Notes in Economics and Mathematical Systems 396, Applied Simulated Annealing*, Springer-Verlag, New York, 1993, pp. 17–44.

[4]Gallego, R. A., Alves, A. B., Monticelli, A. A., and Romero, R., "Parallel Simulated Annealing Applied to Long Term Transmission Network Expansion Planning," *IEEE Transactions on Power Systems*, Vol. 12, No. 1, 1997, pp. 181–189.

[5]Goldberg, D. E., *Genetic Algorithms in Search, Optimization and Machine Learning*, Addison Wesley Longman, Reading, MA, 1989, pp. 27–145.

[6]Bianchini, R., and Brown, C., "Parallel Genetic Algorithms on Distributed-Memory Architectures," Computer Science Dept., Univ. of Rochester, TR 436, New York, May 1993.

[7]Cantú-Paz, E., "A Survey of Parallel Genetic Algorithms," Illinois Genetic Algorithms Lab., Univ. of Illinois at Urbana–Champaign, Rept. 97003, May 1997.

[8]Doorly, D. J., Peiro, J., and Spooner, S., "Design Optimisation Using Distributed Evolutionary Methods," AIAA Paper 99-0111, Reno, NV, USA, 11–14 Jan. 1999.

[9]Wang, X., and Damodaran, M., "Aerodynamic Shape Design Optimization Using Computational Fluid Dynamics and Parallel Simulated Annealing Algorithms," *AIAA Journal*, Vol. 39, No. 8, Aug. 2001, pp. 1500–1508.

[10]Yoon, S., and Kwak, D., "Implicit Navier–Stokes Solver for Three-Dimensional Compressible Flows," *AIAA Journal*, Vol. 30, No. 11, 1992, pp. 2653–2659.

[11]Yee, H. C., and Harten, A., "Implicit TVD Schemes for Hyperbolic Conservation Laws in Curvilinear Coordinates," *AIAA Journal*, Vol. 25, No. 2, 1987, pp. 266–274.

[12]Bhandarkar, S. M., and Machaka, S., "Chromosome Reconstruction from Physical Maps Using a Cluster of Workstations," *Journal of Supercomputing*, Vol. 11, No. 1, 1997, pp. 61–87.

[13]van Laarhoven, P. J. M., and Aarts, E. H. L., *Simulated Annealing: Theory and Applications*, Kluwer Academic, Norwell, MA, 1987, pp. 139–148.

[14]Witte, E. E., and Franklin, M. A., "Parallel Simulated Annealing Using Speculative Computation," *IEEE Transactions on Parallel and Distributed Systems*, Vol. 2, No. 4, 1991, pp. 483–493.

[15]Press, W. H., Teukolsky, S. A., Vetterling, W. T., and Flannery, B. P., *Numerical Recipes in Fortran: The Art of Scientific Computing*, 2nd ed., Press Syndicate of Univ. of Cambridge, Cambridge Univ. Press, U.K., 1997, pp. 107–122.